Barbara Helizanowicz[1,2*], Damian Helizanowicz[2], Łukasz Krzemiński[3], Grzegorz Matula[3]

[1] WB Centrum Kompozytów sp. z o.o., ul. Nad Białką 25, 43-502 Czechowice Dziedzice, Poland
[2] Silesian University of Technology, Faculty of Materials Engineering, ul. Z. Krasińskiego 8, 40-019 Katowice, Poland
[3] Silesian University of Technology, Faculty of Mechanical Engineering, ul. S. Konarskiego 18A, 44-100 Gliwice, Poland
*Corresponding author: E-mail: b.helizanowicz@gmail.com

USE OF COMPUTED TOMOGRAPHY TO ASSESS QUALITY AND STRUCTURE OF CURVED CFRP LAMINATE SAMPLES PRODUCED BY AUTOCLAVE TECHNOLOGY

Carbon fiber reinforced polymer (CFRP) composite laminates are widely used in parts with complex shapes with different curvatures. The curved regions are susceptible to the occurrence of manufacturing defects and premature in-service damage, thus the nondestructive inspection (NDI) of the curved regions is an important issue. X-ray computed tomography (CT) was used to assess the structure of CFRP composite laminate curved beams with different curvature geometry produced in the autoclave technology. The performed inspection allowed visualization of the structure of the curvatures on the ply level and the detection of defects such as foreign objects, voids, resin rich regions, wrinkles and changes in thickness. Also, the quantitative assessment of the defects and distances between the adjacent layers was carried out. The performed investigations show that X-ray CT is an adequate tool to visualize curved CFRP structures.

Keywords: CFRP, curved laminate, autoclave technology, NDI, computed tomography

INTRODUCTION

CFRP is widely used as a lightweight construction material in the military, automotive and aerospace industry. Thanks to its high specific density and specific stiffness, it allows excellent properties to be obtained with a simultaneous reduction in mass. It leads to major benefits such as an increase in speed and the capacity or reduction of fuel consumption of vehicles [1-3].

One of the most common methods of producing composite parts for the aerospace industry is autoclave technology. This method enables the production of high quality parts with limited defects and high mechanical properties. Autoclave curing also provides repeatability, dimensional stability and a high fiber volume fraction. The main raw materials in this process are prepregs composed of fibers pre-impregnated with B-stage (partially cured) resin [4-6].

Numerous applications require a curved laminate shape, for example, airplane fuselage and wings, boat hulls, wind turbine blades, C-section or L-section spars, gear housings, etc. [7-9]. Curved regions are critical for the safe operation of composite structures. In fact, sometimes premature or sudden failure occurs in the curvature, caused by out-of-plane loading. Analyses of curved areas are complex as most laminate theories refer to flat plates and in-plane loading [8, 10-15].

Moreover, corners and curvatures are regions where there is an increased risk of manufacturing defects. A wide range of non-conformities may appear, such as reinforcement deformations, voids, resin rich areas, wrinkles, corner thinning or thickening and spring-in [16-18].

It was proven that these defects strongly influence the strength under out-of-plane loading [7, 15, 19-23]. All these reasons make non-destructive inspection a very important issue related to curved laminate manufacturing and in-service checking.

There are several established methods of NDI suitable for CFRP composite laminates: ultrasonic testing (UT), eddy current testing (ECT), infrared thermography (IrNDT), shearography, acoustic emission and X-ray computed tomography (CT) [24-26].

The X-ray CT method has been intensively developed in recent years and its application and possibilities have significantly grown. This method is based on an X-ray beam which scans a sample placed on a rotary table at many different angles. Differences in the X-ray paths are then captured by detectors and the acquired radiographs are processed by the reconstruction software to create a 3D image of the inspected object [27-29].

X-ray CT is an effective method of composite NDI as it allows 3D data concerning fiber architecture, defects, void content or utilization damage to be received [28-31]. CT has already been used to investigate the deformation of different glass fiber preforms (classic, stitched and 3D) during the manufacture of curved plates with resin transfer molding [7]. It has also been employed to inspect sandwich honeycomb composites with a planar but curved shape [32]. In another study, CT was utilized to detect delamination caused by bending in curved CFRP beams [33].

In this study, X-ray CT was used to visualize a microstructure and detect manufacturing defects in CFRP composite laminate beams with different curvatures produced by the autoclave technique.
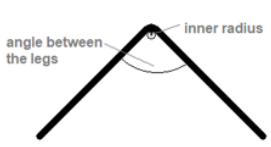
MATERIALS AND METHODS

Samples were made with a high strength carbon-epoxy prepreg employing autoclave technology. Two types of UD prepreg were utilized to consider different ply thicknesses in the curved area: thin ply (TP) and standard ply (SP). The areal weight of the thin ply was 75 gsm (grams per square meter) and 150 gsm for the standard ply. All the prepreg components and parameters were the same for both the materials except the areal weight and the resin content, which was 37.5% for the thin ply and 32.3% for the standard ply prepreg. The manufacturing procedure was conducted in the WB Centrum Kompozytów company facility. The technological details are protected by commercial confidentiality.

In order to investigate the influence of the geometry on composite curvature quality, samples were produced as curved plates with different angles between the legs and a different inner radius but with a 250 mm sample length in each case. The angles and radii are given in Table 1.

TABLE 1. **Geometry of curved samples for CT inspection**

Angle between legs	Inner radius [mm]	
150°	4; 36	
120°	4; 36	
90°	4; 12; 36	

The TP samples were made of 26 layers and the SP samples were made of 13 layers and the same, unidirectional orientation ([0°] – parallel to the curvature). All the samples were produced by the hand lay-up method and cured in one autoclave process. After curing, 15 mm wide beams were cut out from the middle of the plates. For each geometry, one TP and one SP specimen was examined by X-ray CT. The produced samples were a part of a broader investigation regarding the use of thin ply prepregs for curved composite parts [34]. A general overview of the curved beams is shown in Figure 1. The CT inspection of the curved specimens was performed at the Faculty of Mechanical Engineering of the Silesian University of Technology. The scans were performed by a Nikon XT H 225 St 2x computed tomography scanner. The specimens were placed on extruded polyester supports. X-ray emission was generated by a molybdenum anode. The CT scans of the specimens were acquired at 60kV voltage and 4W power. A CsI:Tl detector with the dimensions 43 x 43 cm and 2850 x 2850 pixel resolution was used. The scans were obtained by rotating the specimen by an angle of 210° performing 2800 projections with 8 frames per projection and a 125 ms acquisition time for one frame. The 3D reconstruction of the inspected specimens was performed by means of Nikon CT Pro 3D and VG Studio MAX 2023.2. software.
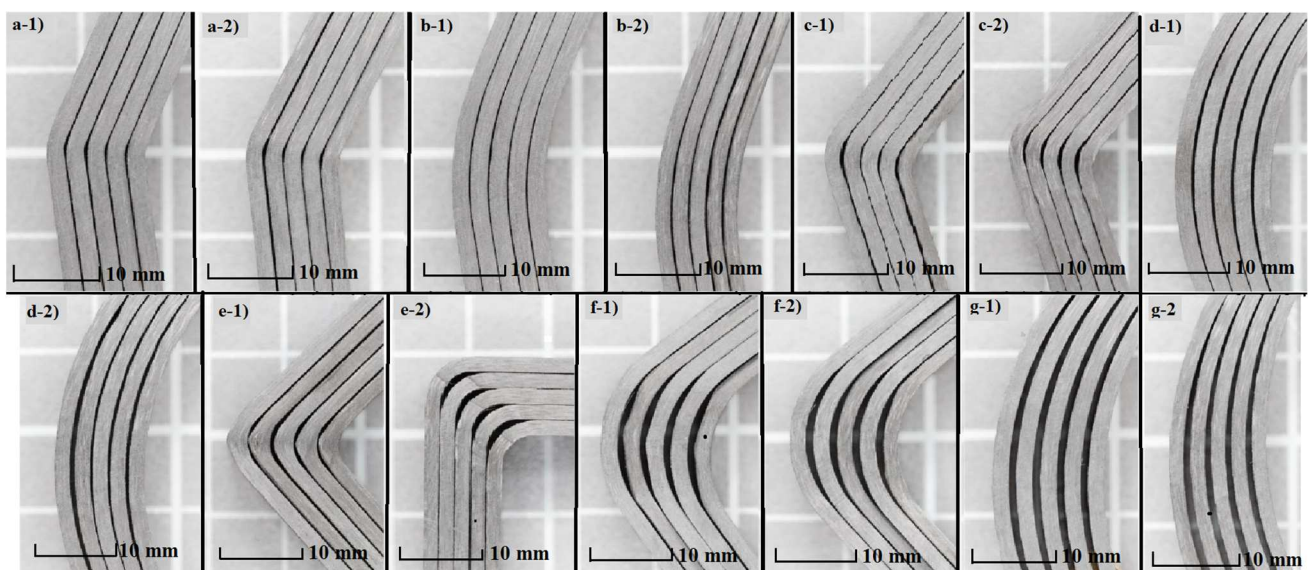

Fig. 1. General overview of manufactured curved beam specimens: 1) thin ply specimens; 2) standard ply specimens; a) 150° angle and 4 mm inner radius; b) 150° angle and 36 mm inner radius; c) 120° angle and 4 mm inner radius; d) 120° angle and 36 mm inner radius; e) 90° angle and 4 mm inner radius; f) 90° angle and 12 mm inner radius; g) 90° angle and 36 mm inner radius

RESULTS

The conducted CT inspection enabled a complete 3D visualization of the curved beam structure to be obtained, including the fiber architecture (especially around the curvature), the distance of adjacent plies, the occurrence and size of defects such as voids, foreign objects, resin rich areas and wrinkles. An example of a 3D view of an investigated structure is shown in Figure 2.
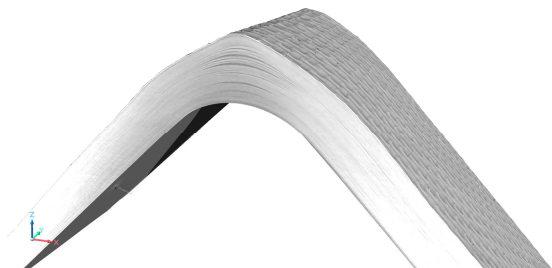

Fig. 2. 3D visualization of curved beam structure: TP specimen with 90° angle and 4 mm inner radius

The general information about the structure based on the CT scans is that the manufactured specimens were characterized by good quality with small distances between the plies, filled with resin and no porosity. However, a few types of defects were detected. One of them was interlayer voids, which are visible as black spots (Fig. 3). Only a few voids were detected in two of the examined specimens (both in the TP and SP specimens of the same geometry – 90° angle and 4 mm inner radius, which is the sharpest shape of all the curved beams). The dimensions of all the detected voids were measured employing ImageJ software, and in each case their size was smaller than the single ply thickness.
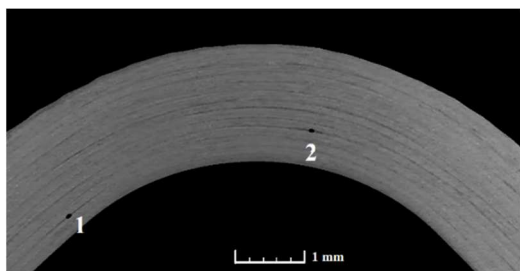

Fig. 3. Interlayer voids detected in SP specimen with 90° angle and 4 mm inner radius (dimensions: 1 – 0.085 mm x 0.043 mm; 2 – 0.091 mm x 0.051 mm)

Another issue detected in the CT images were foreign objects between the layers, visible as white spots (Fig. 4). Their possible source might be residuals of the release foil, silicone paper or other process component remains which adhered to the prepreg during lay-up, but based on the CT scans it was not possible to define their origin. The dimensions of the detected objects were measured by means of ImageJ software and their size was smaller or similar to the single ply thickness, which means that they might have been difficult to notice and remove during the layup.
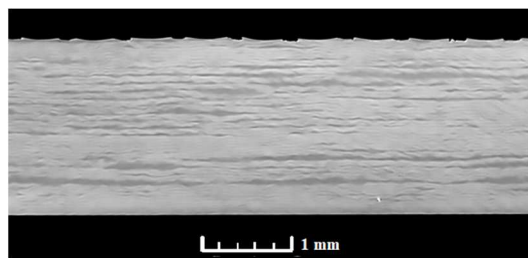
Fig. 4. Foreign object detected in TP specimen with 90° angle and 4 mm inner radius (dimensions: 0.049 mm x 0.028 mm)

After the curing in the autoclave, some wrinkles appeared on the outer surface of the curved regions of the specimens listed in Table 2. The performed CT scans enabled us to take a look inside the wrinkles. In most cases, the wrinkles were rather superficial with a depth negligible compared to the sample thickness and affected only a single or a few outer layers (Fig. 5). Based on the CT images, it was also noticed that the wrinkles were more severe in the TP specimens than in the SP ones – the number and depth of wrinkles were higher in the case of the thin ply (Fig. 6).

TABLE 2. **Specimens with wrinkles on outer surface**

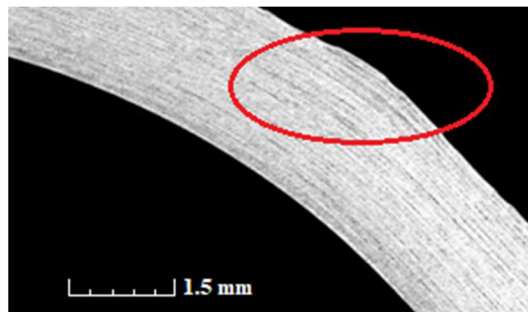| Angle between legs	Inner radius [mm]	
	TP	SP
150°	36	36
120°	4; 36	36
90°	4; 12; 36	12; 36

Fig. 5. Wrinkle on outer surface of TP specimen with 90° angle and 12 mm inner radius
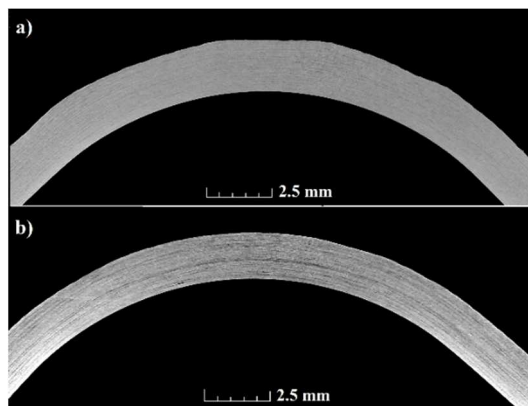

Fig. 6. Comparison of wrinkles present in specimens with 90° angle and 36 mm inner radius: a) TP specimen, b) SP specimen

The next issues revealed by the CT scans were the greater distances between the adjacent layers around the curvature in the curved beams with the 4 mm inner radius. This phenomenon was severe in the specimens with the 90° angle and slightly visible also in the specimens with the 120° angle. Resin rich areas occurred between the layers. Regions with greater amounts of resin occurred in the TP specimens, as shown in Figure 7. The CT micrographs also allowed easy detection of a change in thickness in the curvature and determination of its nature. The change in thickness is visible in Figures 6 and 7.

The mean distance between the adjacent layers for the curved beams with the 4 mm inner radius was determined using ImageJ software by measuring the 5 visibly highest and 5 visibly smallest distances. The results are presented in the Table 3.

TABLE 3. **Mean distance between adjacent layers in curved beams with 4 mm inner radius**

Angle between legs	Mean distance between adjacent layers [mm]	
	TP	SP
90°	0.0331	0.0184
120°	0.0106	0.0094
150°	0.0134	0.0118

The results confirm that enlarged interlayer regions are the highest for the 90° specimens. Another observation is that in each case the distances are higher for the TP specimens than in the SP ones although on the CT scans the microstructure seems to be more uniform for the TP specimens as the interfaces of the particular layers are less clear.

DISCUSSION

The larger distances between the adjacent layers in the TP specimens are probably caused by a higher resin content in the raw prepreg material. Better visibility of the interfaces between the layers in the SP specimens may be a result of the higher bending stiffness of the prepreg material, which caused less deformation of particular layers [34]. Nevertheless, the contrast and resolution of the scans may also influence this phenomenon. The TP specimens have a doubled number of plies, hence higher resolution may be required to clearly visualize the interlayer interfaces. Low contrast between the resin and fibers is also a known problem in the X-ray CT of CFRP composite laminates due to the small difference in the attenuation coefficient [31].

The acquired micrographs are sufficient enough to evaluate the quality and structure of the manufactured samples with special attention to the curvatures. The main manufacturing defects such as foreign objects, voids and resin rich regions were detected. The fiber architecture was also visualized, but rather on the ply level. The performed CT inspection did not allow us to reach the level of single fibers as it requires a higher resolution. It was also impossible to determine the void content based on the scans owing to the lack of contrast. These details require other inspection parameters. Despite that, the investigations provided comprehensive data about the structure of curved CFRP composite laminate beams; therefore, it seems to be a useful method for inspecting large composite parts with complex geometry as the ply level enables assessment of most of the manufacturing defects. More detailed visualization requires limited specimen dimensions, which may be problematic with real industry parts.
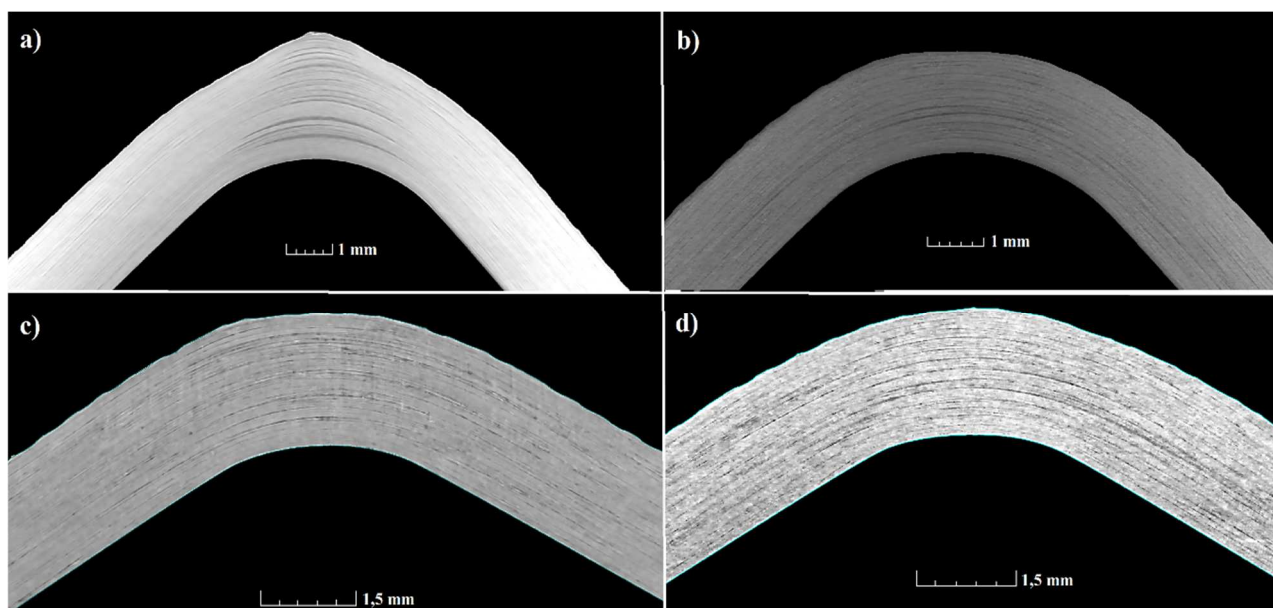

Fig. 7. Resin rich regions between layers around curvature in specimens: a) TP with 90° angle and 4 mm inner radius, b) SP with 90° angle and 4 mm inner radius, c) TP with 120° angle and 4 mm inner radius, d) SP with 120° angle and 4 mm inner radius

Another option for more detailed images is partial scanning and reconstruction to provide a full object image, but it is a very time-consuming process.

CONCLUSIONS

Curved CFRP composite laminate beams with different curvature geometry manufactured utilizing autoclave technology were examined by means of X-ray computed tomography. The inspection of specimens made of thin ply and standard ply prepregs was performed with the same parameters. The conducted inspection allowed detection of all the manufacturing defects, including foreign objects, voids, resin rich regions and wrinkles, which are the most common defects of curved composite parts. The images of the structure were clearer for the specimens made of the standard ply prepreg, which had half the number of thin ply samples layers.

The CT scans acquired in the performed study allowed visualization of the fiber architecture on the ply level. To reach the single fiber level, higher resolution is required. It may be gained with other parameters of investigation, smaller sized specimens or partial scanning with 3D reconstruction. Nonetheless, in most cases the ply level is sufficient to assess part quality. The obtained results enabled visualization of the structure and detection of all the defects which occurred in the curved regions. As the performed study shows, X-ray CT is a good method to evaluate the structure of curved composites, thus it is an NDI tool adequate for CFRP composite laminates of complex shapes.

Acknowledgements

REFERENCES

[1] Wu C., Xu F., Wang H., Liu H., Yan F., Ma C., Manufacturing technologies of polymer composites – A review, Polymers 2023, 15, 712, DOI: 10.3390/polym15030712.

[2] Koniuszewska A., Naplocha K., Kaczmar J.W., Zastosowanie lekkich elementów z kompozytów polimerowych i metalowych w budowie środków transportu, TTS Technika Transportu Szynowego 2015, 22, 12, 2650-2656.

[3] Muhammad A., Rahman M.R., Baini R., Bin Bakri M.K., Applications of sustainable polymer composites in automobile and aerospace industry, Advances in Sustainable Polymer Composites 2021, 185-207, DOI: 10.1016/b978-0-12-820338-5.00008-4.

[4] Mallick P.K., Fiber-Reinforced Composites, Materials, Manufacturing, and Design, 3rd ed., CRC Press, Boca Raton 2007, DOI: 10.1201/9781420005981.

[5] Królikowski W., Polimerowe kompozyty konstrukcyjne, Wydawnictwo Naukowe PWN, Warszawa 2012.

[6] Hubert P., Fernlund G., Poursartip A., Autoclave processing for composites, Manufacturing Techniques for Polymer Matrix Composites (PMCs), Woodhead Publishing Series in Composites Science and Engineering 2012, 414-434, DOI: 10.1533/9780857096258.3.414.

[7] Kozioł M., Mechanical performance of GFRP laminates manufactured from deformed stitched and three-dimensional woven preforms, Journal of Composite Materials 2016, 50, 19, 2617-2631, DOI: 10.1177/0021998315609975.

[8] Chiang Y.-Ch., Curved laminate analysis, Structural Engineering and Mechanics 2011, 39, 2, 169-186, DOI: 10.12989/sem.2011.39.2.169

[9] Figlus T., Kozioł M., Kuczyński Ł., Impact of application of selected composite materials on the weight and vibroactivity of the upper gearbox housing, Materials 2019, 12, 2517, DOI: 10.3390/ma12162517.

[10] MIL-HDBK-17-3F: Department of Defense Handbook. Composite materials handbook. Volume 3. Polymer Matrix Coposites. Materials Usage, Design and Analysis, United States of America Department of Defense, 17 June 2002.

[11] Aggarwal M., Analysis of curved composite beam, Master Thesis, West Virginia University, Morgantown, December 2016.

[12] Kedward K.T., Wilson R.S., McLean S.K., Flexure of simply curved composite shapes, Composites 1989, 20, 6, 527--536, DOI: 10.1016/0010-4361(89)90911-7.

[13] Yavuz B.O., Parnas L., Coker D., Interlaminar tensile strength of different angle-ply CFRP composites, Procedia Structural Integrity 2019, 21, 198-205, DOI: 10.1016/j.prostr.2019.12.102.

[14] Martin R.H., Delamination failure in unidirectional curved composite laminate, NASA Contractor Report No. 182018, Hampton 1990, April.

[15] Zumaquero P.L., Justo J., Graciani E., On the thickness dependence of ILTS in curved composite laminates, Key Engineering Materials 2018 August, 774, 523-528, DOI: 10.4028/www.scientific.net/KEM.774.523.

[16] Hassan M.H., Othman A.R., Kamaruddin S., A review on the manufacturing defects of complex-shaped laminate in aircraft composite structures, The International Journal of Advanced Manufacturing Technology 2017, 91, 4081-4094, DOI: 10.1007/s00170-017-0096-5.

[17] Netzel C., Mordasini A., Schubert J., Allen T., Battley M., Hickey C.M.D., Hubert P., Bickerton S., An experimental study of defect evolution in corners by autoclave processing of prepreg material, Composites Part A: Applied Science and Manufacturing 2021, May, 144, 106348, DOI: 10.1016/j.compositesa.2021.106348.

[18] Azzouz R., Allaoui S., Moulart R., Composite preforming defects: a review and a classification, International Journal of Material Forming 2021, 14, 1259-1278, DOI: 10.1007/s12289-021-01643-7.

[19] Seon G., Makeev A., Nikishkov Y., Lee E., Effects of defects on interlaminar tensile fatigue behavior of carbon/epoxy composites, Composites Science and Technology 2013, December, 89, 194-201, DOI: 10.1016/j.compscitech.2013.10.006.

[20] Hakim I.A., Donaldson S.L., Meyendorf N.G., Browning C.E., Porosity effects on interlaminar fracture behavior in carbon fiber-reinforced polymer composites, Materials Sciences and Applications 2017, July, 8, 2, 170-187, DOI: 10.4236/msa.2017.82011.

[21] Costa M.L., M.de Almeida S.F., Rezende M.C., The influence of porosity on the interlaminar shear strength of carbon/epoxy and carbon/bismaleimide fabric laminates,

Composites Science and Technology 2001, November, 61, 14, 2101-2108, DOI: 10.1016/S0266-3538(01)00157-9.

[22] Bowles K.J., Frimpong S., Void effects on the interlaminar shear strength of unidirectional graphite-fiber-reinforced composites, Journal of Composite Materials 1992, 26, 10, 1487-1509, DOI: 10.1177/002199839202601006.

[23] Makeev A., Seon G., Nikishkov Y., Lee E., Methods for assessment of interlaminar tensile strength of composite materials, Journal of Composite Materials 2014, 49, 7, 783-794, DOI: 10.1177/0021998314525979.

[24] Salski B., Gwarek W., Korpas P., Reszewicz S., Chong A.Y.B., Theodorakeas P., Hatziioannidis I., Kappatos V., Selcuk C., Gan T.-H., Koui M., Iwanowski M., Zielinski B., Non-destructive testing of carbon-fibre-reinforced polymer materials with a radio-frequency inductive sensor, Composite Structures 2015, 122, 104-112, DOI: 10.1016/j.compstruct.2014.11.056.

[25] Wu D., Cheng F., Yang F., Huang C., Non-destructive testing for carbon-fiber-reinforced plastic (CFRP) using a novel eddy current probe, Composites Part B: Engineering 2019, November, 177, 107460, DOI: 10.1016/j.compositesb.2019.107460.

[26] Chen J., Yu Z., Jin H., Nondestructive testing and evaluation techniques of defects in fiber – reinforced polymer composites: A review, Frontiers in Materials 2022, 9, 986645, DOI: 10.3389/fmats.2022.986645.

[27] Landis E.N., Keane D.T., X-ray microtomography, Materials Characterization 2010, December, 61, 12, 1305-1316, DOI: 10.1016/j.matchar.2010.09.012.

[28] Garcea S.C., Wang Y., Withers P.J., X-ray computed tomography of polymer composites, Composites Science and Technology 2018 March, 156, 305-319, DOI: 10.1016/j.compscitech.2017.10.023.

[29] Gao Y., Hu W., Xin S., Sun L., A review of applications of CT imaging on fiber reinforced composites, Journal of Composite Materials 2022, January, 56, 1, 133-164, DOI: 10.1177/00219983211050705.

[30] Nikishkov Y., Airoldi L., Makeev A., Measurement of voids in composites by X-ray computed tomography, Composites Science and Technology 2013, December, 89, 89-97, DOI: 10.1016/j.compscitech.2013.09.019.

[31] Zwanenburg E.A., Norman D.G., Qian C., Kendall K.N., Williams M.A., Warnett J.M., Effective X-ray micro computed tomography imaging of carbon fibre composites, Composites Part B: Engineering 2023, June, 258, 110707, DOI: 10.1016/j.compositesb.2023.110707.

[32] Liu T., Malcolm A., Xu J., High-resolution X-ray CT inspection of honeycomb composites using planar computed tomography technology, 2nd Int. Symposium on NDT in Aerospace, Hamburg, Germany 22-24, November 2010.

[33] Vavrik D., Jakubek J., Jandejsek I., Krejci F., Kumpova I., Zemlicka J., Visualization of delamination in composite materials utilizing advanced X-ray imaging techniques, Journal of Instrumentation 2015, April, 10, DOI: 10.1088/1748-0221/10/04/C04012.

[34] Helizanowicz B., The use of thin-ply prepregs for the fiber reinforced polymer composites with small radius curvatures manufactured in the autoclave technology, Doctoral thesis, Faculty of Materials Engineering, Silesian University of Technology, Katowice 2023.